

1 Quantifying the soil sink of atmospheric Hydrogen: a full year of field 2 measurements from grassland and forest soils in the UK

3 Nicholas Cowan¹, Toby Roberts¹, Mark Hanlon¹, Aurelia Bezanger¹, Galina Toteva^{1,2}, Alex Tweedie^{1,2}, Karen
4 Yeung¹, Ajinkya Deshpande¹, Peter Levy¹, Ute Skiba¹, Eiko Nemitz¹, Julia Drewer¹

5 ¹UK Centre for Ecology & Hydrology, Easter Bush, Midlothian, UK, EH26 0QB

6 ²School of GeoSciences, The University of Edinburgh, Edinburgh, United Kingdom

7 **Corresponding author:** Nicholas Cowan (nicwan11@ceh.ac.uk)

8 **Keywords:** greenhouse gas, carbon, methane, flux, chamber methodology

9 Abstract

10 Emissions of hydrogen (H_2) gas from human activities are associated with indirect climate warming effects. As
11 the hydrogen economy expands globally (e.g. the use of H_2 gas as a fuel), the anthropogenic release of H_2 into
12 the atmosphere is expected to rise rapidly as a result of increased leakage. The dominant H_2 removal process
13 is uptake into soils; however, removal mechanisms are poorly understood and the fate and impact of
14 increased H_2 emissions remains highly uncertain. Fluxes of H_2 within soils are rarely measured, and data to
15 inform global models is based on few studies. This study presents soil H_2 fluxes from two field sites in central
16 Scotland, a managed grassland and a planted deciduous woodland, with flux measurements of H_2 covering
17 full seasonal cycles. A bespoke flux chamber measurement protocol was developed to deal with the fast
18 decline in headspace concentrations associated with rapid H_2 uptake, in which exponential regression models
19 could be fitted to concentration data over a 7-minute enclosure time. We estimate annual H_2 uptake of -3.1 ± 0.1 and $-12.0 \pm 0.4 \text{ kg } H_2 \text{ ha}^{-1} \text{ yr}^{-1}$ and mean deposition velocities of 0.012 ± 0.002 and $0.088 \pm 0.005 \text{ cm s}^{-1}$
20 for the grassland and woodland sites, respectively. Soil moisture was found to be the primary driver of H_2
21 uptake at the grassland site, where the high silt/clay content of the soil resulted in anaerobic conditions (near
22 zero H_2 flux) during wet periods of the year. Uptake of H_2 at the forest site was highly variable and did not
23 correlate well with any localised soil properties (soil moisture, temperature, total carbon and nitrogen
24 content). It is likely that the high silt/clay content of the grassland site (55% silt, 20% clay) decreased aeration
25 when soils were wet, resulting in poor aeration and low H_2 uptake. The well-drained forest site (60% sand)
26 was not as restricted by exchange of H_2 between the atmosphere and the soil, showing instead a large
27 variability in H_2 flux that is more likely to be related to heterogeneous factors in the soil that control microbial
28 activity (e.g. labile carbon and microbial densities). The results of this study highlight that there is still much

30 that we do not understand regarding the drivers of H₂ uptake in soils and that further field measurements are
31 required to improve global models.

32 **1. Introduction**

33 Prior to the industrial revolution in the 18th century, the atmospheric concentration of Hydrogen gas (H₂) was
34 relatively stable at approximately 330 ppb (Patterson et al., 2021). Human activity over the past two centuries
35 has resulted in increasing atmospheric H₂ concentrations (546 ppb in 2021, Petron et al. (2023)), partly as a
36 result of increasing industrial leaks (Hitchcock 2019; Cooper et al., 2022), partly due to increases in emissions
37 and concentrations of precursor gases such as methane (CH₄) and volatile organic compounds (VOCs), and
38 partly due to increasing concentrations of other gases in the atmosphere which extend the natural lifetime
39 of H₂ (Patterson et al., 2021). In the atmosphere, H₂ competes for hydroxyl (OH) radicals with gases such as
40 methane (CH₄) and carbon monoxide (CO), thus an increase in concentrations of these gases due to human
41 activities has resulted in increasing competition for OH and extended the lifetimes for each species (Khalil &
42 Rasmussen, 1990; Bertagni et al., 2022). Concentrations of atmospheric H₂ gas are indirectly associated with
43 climate warming effects as a result of extending the atmospheric lifetime of the powerful greenhouse gas CH₄
44 as well as increasing tropospheric ozone and stratospheric water vapour, which also have a warming potential
45 (Warwick et al., 2004; Ocko & Hamburg, 2022). The associated indirect global warming potential (GWP) had
46 been estimated to be in the range of 3.3 to 5 over a hundred-year time horizon (Derwent et al., 2020, Field &
47 Derwent, 2021), though recent estimates have been made of up to 11.6 ± 2.8 times that of an equivalent
48 mass of carbon dioxide (Sand et al., 2023). The effective GWP and the atmospheric accumulation of H₂ are
49 highly sensitive to its atmospheric lifetime, which is estimated to be approximately 2 years (Novelli et al.,
50 1999).

51 The dominant process for H₂ removal from the atmosphere is uptake by soils, which is estimated to be three
52 times larger than the sink due to atmospheric reaction with OH (Warwick et al., 2004; Derwent et al., 2020;
53 Field & Derwent, 2021; Paulot et al., 2021; Ocko & Hamburg, 2022). Whilst both removal mechanisms are
54 highly uncertain (especially the soil sink), the fate and impact of increased H₂ emissions depends largely on
55 the soil sink strength (Ehhalt & Rohrer, 2009). The microbial uptake of H₂ can occur both under aerobic and
56 anaerobic conditions, but the global atmospheric H₂ sink is dominated by processes that occur in aerobic soils
57 at the atmosphere-biosphere interface (soil surface) where atmospheric H₂ availability is not as limited (Piché-
58 Choquette & Constant, 2019). A large spectrum of bacteria and archaea can utilise H₂ as an energy source,
59 via the hydrogenase enzyme. Whilst some investigations have highlighted the importance of high-affinity H₂-
60 oxidising bacteria (Saavedra-Lavoie et al., 2020), most studies suggest that this enzyme is widespread across
61 many bacterial and archaeal phyla, and that H₂ consumption is the norm rather than the exception (Islam et

62 al., 2020; Greening & Grinter, 2022). Studies investigating specific H₂ uptake rates for different soil types and
63 conditions have been carried out but are sparse and limited to a small number of geographies (primarily
64 North America, Europe and Japan, e.g., Yonemura et al., 1999; Yonemura et al., 2000; Smith-Downey 2008;
65 Lallo et al., 2009; Hammer and Levin, 2009; Khodhiri et al., 2015). In addition to microbial activity, diffusion
66 into the soil is a further important rate limiting step (Bertagni et al., 2021). Gases penetrate the soil by passive
67 diffusion and diffusion rates are mainly influenced by porosity, which is affected by soil structure, texture,
68 organic matter contents, vegetation types (roots) and moisture content. Thus, for the same microbial activity,
69 porous soils can be expected to be much larger H₂ sinks than compacted and/or waterlogged soils due to
70 increased gas exchange rates with the atmosphere. At the larger scale, diffusion rates will depend on the
71 changing climate: a wetter climate may lower the H₂ diffusion rates (Paultot et al., 2021). Temperature is
72 another important factor as it determines the rate of microbial enzyme reactions and in addition a carbon
73 source is also required for heterotrophic microbial activity (Islam et al., 2020; Meredith et al., 2016; Baril et
74 al., 2022). The biological sink of atmospheric H₂ has been suggested to be more sensitive to spatial variations
75 of drivers (specifically microbial diversity) compared to the fluxes of other gases with high variability such as
76 nitrous oxide (N₂O) (e.g. Baril et al., 2022); however, studies reporting the spatial variability of H₂ fluxes in
77 soils are limited.

78 Historically, the processes that control H₂ uptake in soils have been severely understudied due to the logistical
79 difficulties and technical constraints on measuring H₂ fluxes. This study presents measurements of H₂ fluxes
80 between the soil and the atmosphere at two field sites in central Scotland, a managed grassland and a planted
81 deciduous woodland. These are the first reported flux measurements of H₂ covering a full annual cycle in the
82 UK. It has previously been reported that forest ecosystems exhibit higher H₂ uptake rates than agroecosystems
83 (Ehhalt and Rohrer, 2009); however, the generality of this and exact mechanisms are still unclear. This study
84 aims to investigate the response of microbial H₂ uptake at a grassland and a forest site to environmental
85 drivers, and to identify differences between the sites. We also describe a dedicated flux chamber
86 methodology which has been developed to best address the challenges of measuring H₂ flux using gas
87 chromatography (GC) analysers.

88

89 **2. Methods**

90 **2.1. Field Sites**

91 Measurements of trace gas fluxes and environmental variables were made at two field sites within the
92 Midlothian region in central Scotland (UK, approximately 6 miles south of Edinburgh, Table 1). The first of
93 these was the long-term environmental monitoring site at Easter Bush Farm (grassland). The grassland site

94 (55.8653 °N, -3.206 °W) is an intensively managed, improved grassland (South field in Cowan et al., 2020 and
95 Drewer et al., 2016) that since 2001 has been used predominantly to graze sheep, with a species composition
96 of >99% perennial ryegrass (*Lolium perenne*). The soil type is an imperfectly drained Eutric Cambisol with silt
97 loam soil. The field management is typical for this region, with predominately ammonium nitrate (AN)
98 fertilisation via tractor-mounted broadcast spreading, with liming every 3 – 5 years to maintain the pH
99 between 5.5 and 6.0 and occasional ploughing and reseeding. The sheep were absent from the fields in the
100 winter months (November to February), with sporadic movement between local fields throughout the
101 growing season (March to September) as management required. During the period of 01/10/23 to 01/10/24,
102 the cumulative rainfall at the grassland site was 1133 mm and the mean temperature was 8.6 °C which is
103 fairly typical of the site (Table 1)

104 The second field site was a temporary experimental area setup in Glencorse Forest (woodland). Glencorse
105 Forest (55.8540°N, -3.215°W) was converted to a planted deciduous forest from a pasture approximately 40
106 years prior to measurements (Billington and Pelham, 1991). The study plot is situated in a plantation of Silver
107 Birch (*Betula pendula*) and Downy Birch (*Betula pubescens*), with a ground flora consisting mostly of grasses.
108 The soil is classified as a sandy loam which lies under a thin layer (5 – 10 mm) of organic debris. The field site
109 had been subject to enhanced nitrogen deposition with ammonia for approximately 2 years before H₂ flux
110 measurements were carried out (Deshpande et al., 2024). During the period of 01/10/23 to 01/10/24, the
111 cumulative rainfall at the woodland site was 1047 mm and the mean temperature was 9.6 °C which was
112 slightly wetter and warmer than historical mean data (Table 1).

113 **Table 1** Field site environmental properties as reported in previous studies and ongoing research. Mean
114 annual values taken from 10+ years of site data. Rainfall represents throughfall (e.g. rain that reaches the
115 soil).

Property	Easter Bush Farm	Glencorse Forest
Management	Improved grassland (grazed)	Planted woodland (Birch)
Abbreviation	Grassland	Woodland
Soil Type	Mineral	Mineral
Carbon Content (% mass)	4.0	3.1
pH	5.5	5.3
Bulk Density (g cm ⁻³)	1.11	0.96
Particle Density (g cm ⁻³)	2.57	2.34
Sand/silt/clay (%)	25/55/20	60/15/25
Mean Annual Temperature (°C)	8.4	9.0
Mean Annual Rainfall (mm)	1040	920

117 **2.2. Meteorological and soil measurements**

118 Continuous environmental measurements were made at both field sites. Air temperature, soil temperature,
 119 soil volumetric water content (VWC) at three depths (5, 10 and 20 cm at the grassland site; 5, 10 and 15 cm
 120 at the woodland site), relative humidity (RH) and rainfall were measured at both sites throughout the flux
 121 measurement campaign (Table S1). For each flux chamber measurement, soil temperature and soil VWC were
 122 also measured next to the chamber (<0.5 m distance) at the time of the flux measurement. Soil temperature
 123 was measured at 10 cm depth using a handheld probe (ETI Ltd., Worthing, UK), and soil VWC was measured
 124 at 12 cm depth using an HS2 HydroSense II handheld soil moisture sensor (Campbell Scientific, Utah, USA),
 125 with 4 replicates for each chamber. Soil samples were collected for total carbon (C) and total nitrogen (N)
 126 analysis from the top 10 cm of soil at the woodland site in March 2021, September 2021, May 2022, August
 127 2022, November 2022, and March 2023. Subsamples were dried at 105 °C until constant weight, milled using
 128 a ball mill (MM200 ball mill, Retsch, Haan, Germany) and analysed using an elemental analyser (Flash SMART,
 129 Thermo Fisher Scientific, MA, USA).

131 **2.3. Flux measurements**

132 Fluxes of hydrogen (H₂), methane (CH₄) and nitrous oxide (N₂O) were measured using the static chamber
 133 method (e.g. Drewer et al., 2016). Chambers (diameter = 40 cm, height = 30 cm) consisting of opaque
 134 polypropylene open-ended cylinders, were installed at each field site: 20 at Easter Bush (grassland) and 20 at
 135 Glencorse (woodland). The chambers were inserted into the ground to a depth of approximately 10 cm for
 136 the entire study period (chamber air volume of approximately 0.025 m³). The depth to the surface in each
 137 chamber was measured at 5 points on the sides of the chamber base using a ruler, from which the average
 138 was used to calculate the volume of air within. During measurement periods, aluminium lids were fastened
 139 onto the bases using four strong clips; a strip of draft excluder glued onto the lid provided a gas tight seal
 140 between chamber and lid. A three-way tap was used for gas sample removal using a 100 ml syringe. 20 ml
 141 glass vials were filled with a double needle system to flush the vials with five times their volume. Storage tests
 142 using gas standards revealed that gases stored in the vials were stable for up to 24 hours, after which H₂
 143 leakage could be observed in the data. Hence all analyses of H₂ gas samples from the chambers were carried
 144 out within 24 hours of measurement in the field (typically within 6 hours). Measurements of H₂ and GHGs
 145 were made approximately monthly.

146 Two separate measurement protocols were employed to measure greenhouse gases (GHGs) and H₂ fluxes,
 147 due to the differences in how the gases behaved within the chamber over a given timespan. For GHG

148 measurements, the standard practice of extracting four gas samples (100 ml) at regular intervals over one
149 hour (0, 20, 40, 60 min) was used (Drewer et al. 2017). However, due to the rapid uptake of H₂ observed in
150 trial measurements (H₂ in the chamber headspace could reach zero ppb in under 10 mins), the time-evolution
151 of H₂ in the chamber was non-linear and therefore a separate measurement protocol was developed for H₂
152 fluxes. Fluxes of H₂ were measured during entirely separate enclosure periods to the GHGs (albeit on the
153 same day) using an enclosure period with 6 samples taken over 7 minutes (0, 1, 2, 3, 5 & 7 mins). Chambers
154 used to measure H₂ were fitted with a small 5 cm diameter PC fan which ran from a 9 V battery during chamber
155 enclosure times to ensure rapid air mixing over the shorter measurement period.

156 Concentrations of H₂ were measured using an Agilent 8890 gas chromatograph fitted with a pulsed discharge
157 helium ionization detector (GC-PDHID) equipped with a 7697A headspace autosampler, with capacity for 108
158 vials (Agilent, Santa Clara, California, USA). Concentrations of CH₄ and N₂O were measured using a gas
159 chromatograph (Agilent 7890B with headspace autosampler 7697A with capacity for 108 vials; Agilent, Santa
160 Clara, California, USA) with a micro-electron capture detector (μ ECD) for N₂O analysis and flame ionization
161 detector (FID) for CH₄ analysis run in parallel. Each analytical run of H₂ and GHG samples included at least
162 three sets of four certified standard concentrations for calibration purposes (certified to \pm 5%). The
163 instrumental noise (σ) of the instruments were 40, 5, and 15 ppb for CH₄, N₂O and H₂, respectively. Based on
164 the methods used, the analytical uncertainty in flux estimates were 0.55, 0.07 and 1.0 nmol m⁻² sec⁻¹ for CH₄,
165 N₂O and H₂, respectively based on the method of Cowan et al. (2025).

166 Fluxes were calculated using linear and non-linear regression methods using the HMR package for the
167 statistical software R (Pedersen et al., 2010). By convention, positive fluxes represent emission from the soil,
168 and negative fluxes indicate that the soil acts as a sink (i.e. uptake). Fluxes of GHGs were all calculated using
169 linear regression, where dC/dt is calculated using the standard line of best fit through the concentration data.
170 As concentrations of H₂ fall exponentially during chamber measurements when soil uptake of H₂ is high, linear
171 regression is not always appropriate. To account for this, fluxes of H₂ were calculated using both linear
172 regression and the HMR model, depending on the magnitude of the rate of change observed in each chamber
173 measurement. The HMR model is a commonly used non-linear model derived by Hutchinson & Mosier (1981)
174 with a negative exponential form of curvature which calculates the rate of change of a gas concentration at
175 $t = 0$. The concentration C at time t is given by Equation 1, where C_0 is the initial concentration, C_{eq} is the value
176 at equilibrium and k is a constant. dC/dt is the initial rate of change in concentration at $t = 0$ in nmol mol⁻¹
177 s⁻¹, calculated using Equation 2.

$$C_t = C_{eq} - (C_{eq} - C_0) \exp(-kt) \quad (\text{Equation 1})$$

179
$$\frac{dC}{dt} = k(C_{eq} - C_o)$$

(Equation 2)

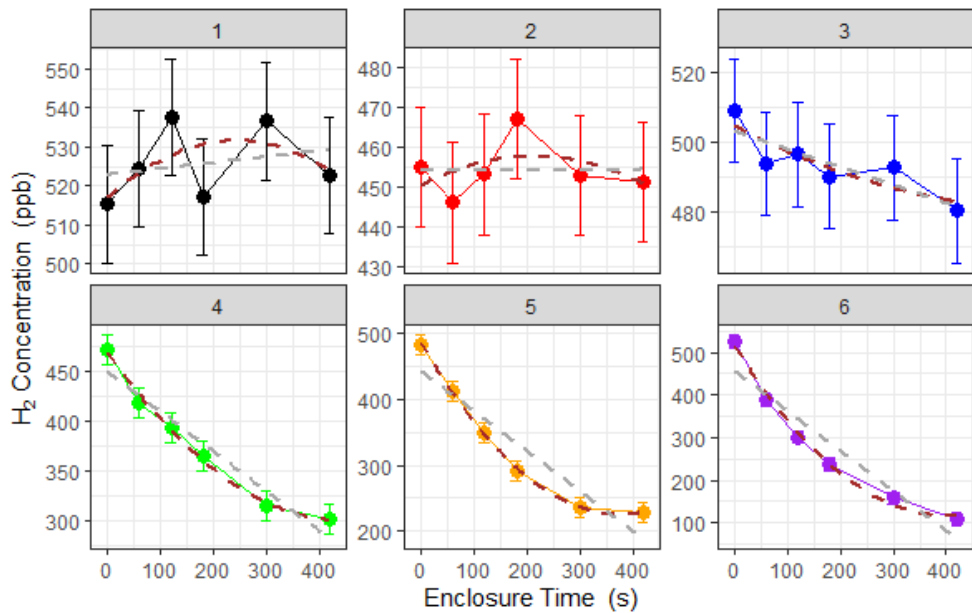
180 The dC/dt at $t=0$ is used to calculate the flux using Equation 3, where F is gas flux from the soil ($\text{nmol m}^{-2} \text{ s}^{-1}$),
 181 ρ is the density of air in mol m^{-3} , V is the volume of the chamber in m^3 and A is the ground area enclosed by
 182 the chamber in m^2 .

183
$$F = \frac{dC}{dt} \times \rho \times \frac{V}{A}$$

(Equation 3)

184 Where soil flux is near the analytical uncertainty of the method (e.g. concentration change within the
 185 chamber is difficult to detect with our instrument), a clear exponential decline was hard to discern from the
 186 measurement noise and could give rise to spurious fits to Equation 1. (Examples 1 and 2 in Figure 1 and Table
 187 2). The criteria for using the HMR model for each individual flux calculation was based on i) k is not
 188 unrealistically large in Equation 2 (as defined and limited by the HMR package in R), ii) the flux estimated by
 189 linear regression is larger than the analytical uncertainty of the method ($1.0 \text{ nmol m}^{-2} \text{ s}^{-1}$ for H_2) and iii) the
 190 95 % confidence interval (95% C.I.) of the HMR model fit is less than 5 times the magnitude of the flux
 191 estimated using linear regression (removes poor-fitting outliers). In Figure 1 and Table 3, six examples are
 192 given in which three selections of linear regression fitting and three selections of the HMR model fitting are
 193 used to determine flux. For large uptake fluxes (Examples 4, 5 and 6) the HMR model provides a more suitable
 194 fit to the non-linearity in dC/dt , which linear regression does not accurately represent. Deposition velocity of
 195 H_2 was calculated by dividing the calculated flux by the ambient concentration at the site (mean of $t = 0$
 196 measurements on day of measurement in mol m^{-3}).

197



198

199 **Figure 1.** Examples of concentration data collected during H₂ flux chamber sampling. Linear regression (grey)
 200 and HM model (brown) are used to determine dC/dt for each chamber measurement. Error bars represent
 201 the instrumental noise of H₂ measurements in GC analysis (15 ppb in this study). Comparisons of flux data
 202 presented in Table 2.

203

204 **Table 2.** Further information on the example data provided in Figure 1. Six examples of chamber H₂ flux
 205 measurements are provided, from the Easter Bush (grassland) and Glencorse (woodland) field sites. The initial
 206 and final concentrations of H₂ within the chamber are provided, as well as the flux and 95% C.I. calculated
 207 using linear and HM model (Equation 2) fitting methods (NA when k is too large). The method selected to
 208 represent the flux in this study based on the described protocols is included.

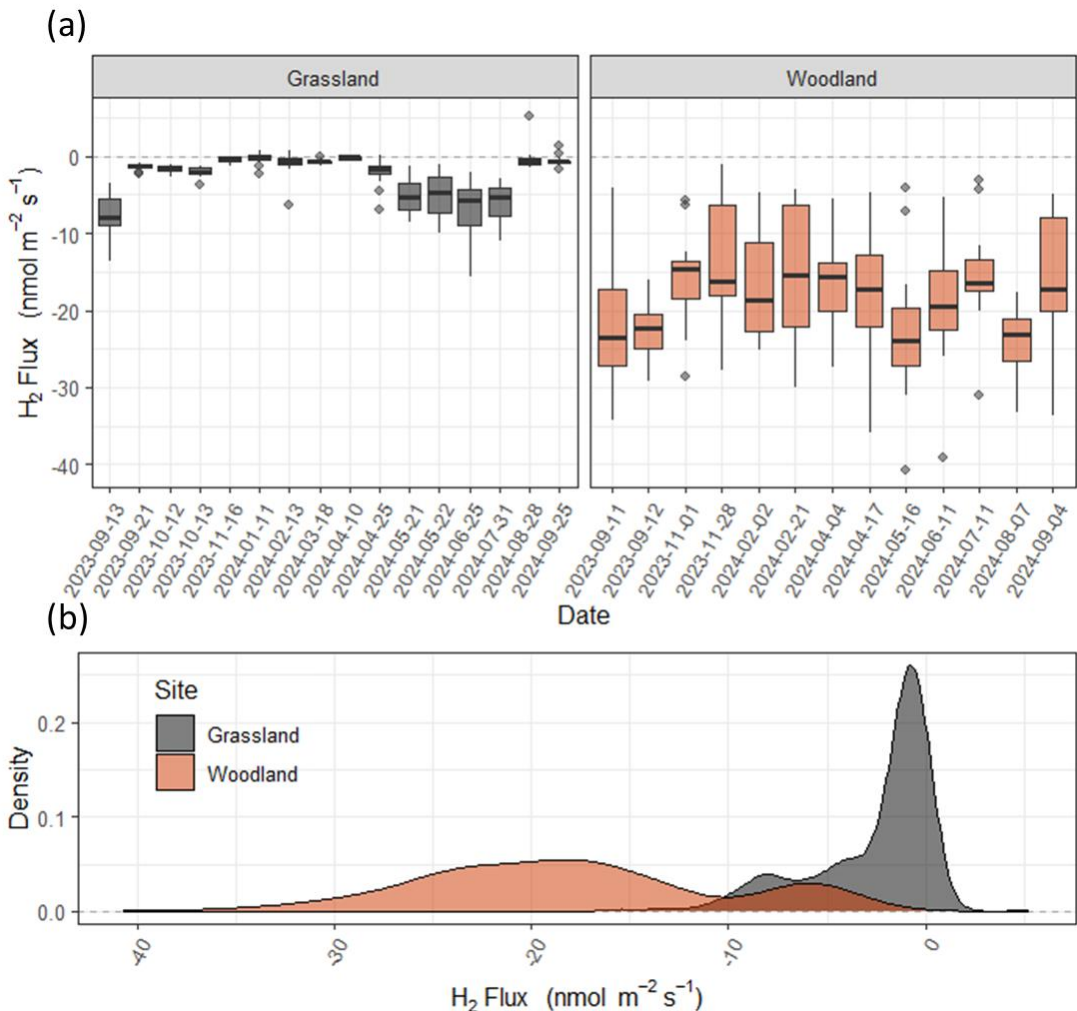
Example	Date	Location	Initial (ppb)	Final (ppb)	Flux Linear fit (nmol m ⁻² s ⁻¹)	Flux HM fit (nmol m ⁻² s ⁻¹)	Selected Method
1	10/04/2024	Grassland	515	522	0.01 (-0.59 – 0.63)	2.839 (NA)	Linear
2	16/11/2023	Grassland	455	451	0.003 (-0.56 – 0.60)	0.239 (-6.47 – 6.99)	Linear
3	13/02/2024	Grassland	509	480	-0.319 (-0.58 – -0.06)	-0.889 (-2.60 – 0.21)	Linear
4	31/07/2024	Grassland	471	300	-3.078 (-4.54 – -3.35)	-6.6 (-9.44 – -3.80)	HM
5	31/07/2024	Grassland	483	229	-3.152 (-4.54 – -3.35)	-10.89 (-15.54 – -6.232)	HM
6	04/04/2024	Woodland	527	109	-5.278 (-7.05 – -1.07)	-14.35 (-15.88 – -12.82)	HM

209

210 **3. Results**

211 **3.1. *Hydrogen Flux measurements***

212 Fluxes of H₂ measured from the grassland site ranged from -15.5 to +5.3 nmol m⁻² s⁻¹ (Figures 2 and S1) over
213 the period of September 2023 to September 2024. More than 90% of the H₂ fluxes measured at the grassland
214 site were negative (soil uptake) and only 2 of 251 chamber measurements showed emissions from the soil
215 which exceed the analytical uncertainty of the method. Fluxes of H₂ at the grassland site changed seasonally,
216 with greater uptake in the spring and summer compared with winter, where the flux was close to zero. Fluxes
217 at the grassland site had a median of -1.2 nmol m⁻² s⁻¹ and 95% percentiles of -9.9 to 0.2 nmol m⁻² s⁻¹. Fluxes
218 measured from the woodland site ranged from -40.7 to -1.1 nmol m⁻² s⁻¹ (Figures 2 and S1). All fluxes
219 measured at the woodland site showed H₂ uptake in the soil. Spatial variability of H₂ flux at the woodland site
220 was an order of magnitude larger than those observed at the grassland site. Fluxes at the woodland site had
221 a median of -18.7 nmol m⁻² s⁻¹ and 95% percentiles of -32.4 to -4.3 nmol m⁻² s⁻¹. Ambient concentrations of H₂
222 at the sites ranged from 424.8 to 566.5 ppb. Mean ambient concentrations at the woodland site (484.4 ppb)
223 were on average 21.7 ppb (4.3 %) lower than the grassland site (506.5 ppb) which could be considered
224 statistically insignificant (t-test, p > 0.1), but differences were fairly consistent throughout the year (summary
225 statistics presented in Table S2).



226

227 **Figure 2.** Fluxes of H₂ measured using the flux chamber method at grassland (Easter Bush, grassland; grey)
 228 and forest (Glencorse Forest, woodland; red) sites in Midlothian, Scotland. Boxplots (a) represent the median,
 229 and 25th and 75th percentiles of flux data of 20 chambers, respectively (whiskers represent the 95th
 230 percentiles). (b) Frequency distributions of the flux data for both sites (Figure replicated for Vd in Figure S1).

231 **3.2. Greenhouse gas fluxes**

232 Fluxes of CH₄ at both sites were close to zero, with mostly small negative fluxes observed at both sites (Figure
 233 S3). Soil uptake of CH₄ was observed during the summer months at both sites but during colder months, only
 234 the woodland site continued to observe consistent negative CH₄ fluxes. Fluxes of CH₄ measured from the
 235 grassland site ranged from -1.2 to 1.0 nmol m⁻² s⁻¹ with a median of -0.14 nmol m⁻² s⁻¹. Fluxes of CH₄ measured
 236 from the woodland site ranged from -1.3 to 2.3 nmol m⁻² s⁻¹ with a median of -0.32 nmol m⁻² s⁻¹. Only 40% of
 237 all CH₄ flux measurements exceeded the analytical uncertainty of the chamber method deployed, highlighting
 238 the magnitude of observed fluxes were near the limit of detection of the methodology. Fluxes of N₂O
 239 measured at both sites were relatively low for all measurement dates (58% of all data below the analytical

240 uncertainty) with the exception of measurements made in April at the grassland site. Nitrogen fertiliser was
241 applied to the field on the 28th of March, resulting in increased N₂O emissions for several weeks (Figure S3).

242

243 **3.3. Drivers of H₂ flux**

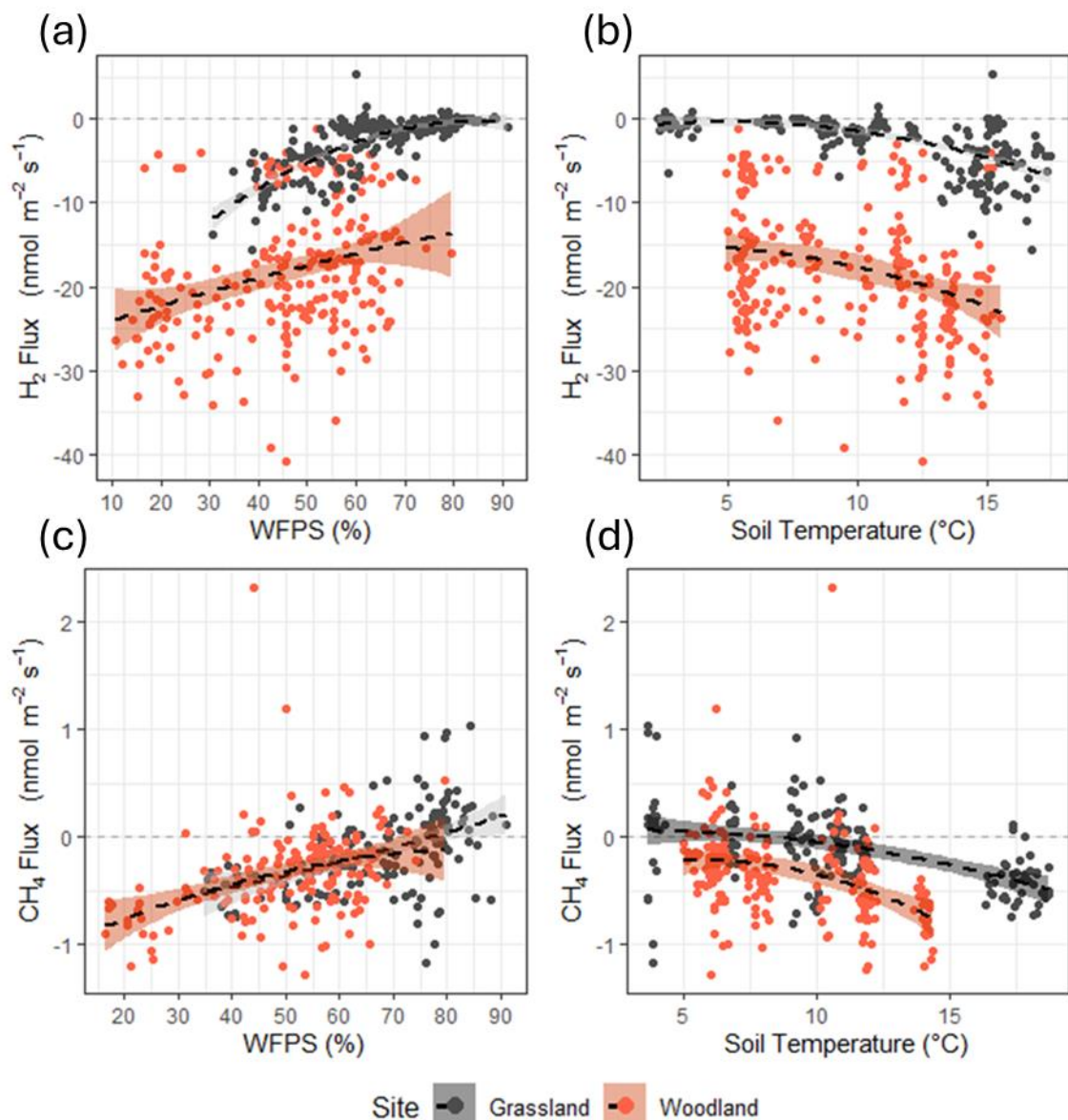
244 Correlations of H₂ flux with soil moisture and soil temperature can be observed at both sites (Figures 4a, 4b
245 and S4); however, each site responds differently. Fluxes of H₂ at the grassland site were close to zero when
246 water filled pore space (WFPS) was high (>45%), then tended towards uptake as WFPS decreased. The
247 correlation between H₂ flux and WFPS is weaker at the woodland site and flux data are widely scattered.
248 Fluxes of H₂ at both the grassland and woodland site tended towards higher uptake as temperature increased,
249 though scatter increased toward higher uptake at both sites (>12 °C). A simplistic multiple regression fit
250 between H₂ flux (y) with soil moisture (x) and soil temperature (z) ($y = a_1x^2 + a_2x + b_1z^2 + b_2z + c$) accounts for
251 more than half of the variance in the observed fluxes at the grassland site ($R^2 = 0.60$) with a significant
252 contribution from soil moisture, but the same approach does not adequately represent the large flux
253 variability at the woodland site ($R^2 = 0.14$) for which neither soil moisture or soil temperature was found to
254 correlate significantly (Table S3). Fluxes of CH₄ at the sites followed the same trends as H₂ flux in terms of
255 emission/uptake and follow similar correlations with soil moisture and soil temperature as H₂ flux (Figures 4c
256 & 4d). Fluxes of CH₄ at both sites were close to zero (or emission) when soils were wet (>45 % WFPS) and cold
257 (<6 °C). Uptake of CH₄ was greatest when soils were drier and warm.

258 . No correlation between H₂ flux with measured total soil C or N in the top 10 cm was found at the woodland
259 site ($R^2 < 0.01$ for each) (Figure S5). Variability in C and N in the replicated cores in the soils in the vicinity of
260 each chamber (< 1 m² distance) was similar to the magnitude of spatial variability observed at the entire plot
261 scale. This suggested a relatively large variability in the soil C and N content at small scales which may
262 obfuscate correlation between soils and fluxes at the individual chamber scale (destructive sampling could
263 not be carried out on soil within the chambers without invalidating flux measurements).

264 By combining continuous soil measurement data collected at each site (soil moisture and temperature at 10
265 cm depth), with the multiple regression model with soil moisture and soil temperature (Figures 4b & 4c) as
266 described in Table S1, continuous H₂ flux predictions were made for a full year (Figure 4a). This model predicts
267 that H₂ flux at the grassland site remains close to zero for most of the time, except when soil moisture drops
268 (e.g. warm months in spring and summer). The model predicts that H₂ flux at the grassland site is strongly
269 dependent on the soil moisture content, with relatively strong periods of H₂ uptake during drier periods
270 (warm periods between rainfall events). H₂ flux estimates at the woodland site are more variable, and less
271 susceptible to changes in meteorology or soil conditions. The model predicts a slowdown in H₂ uptake in the

272 forest soils during the colder months in winter but is not significantly impacted by changing soil moisture.
273 Total annual estimates of H_2 flux predicted by the model are -3.1 ± 0.1 and $-12.0 \pm 0.4 \text{ kg } H_2 \text{ ha}^{-1} \text{ yr}^{-1}$ for the
274 grassland and woodland sites, respectively. By comparison, a straight average of the measurements, without
275 using models to gap-fill the data, suggests mean fluxes (with 95% C.I.s) of -2.6 ± 0.4 and $-18.7 \pm 1.0 \text{ nmol m}^{-2}$
276 s^{-1} which would translate to annual cumulative fluxes of approximately -1.6 ± 0.2 and $-11.7 \pm 0.6 \text{ kg } H_2 \text{ ha}^{-1} \text{ yr}^{-1}$
277 ¹ for the grassland and GC sites, respectively. The two estimates agree well at the woodland site, but the gap
278 filling increases the estimated annual H_2 uptake at the grassland site by 56%.

279



280

281

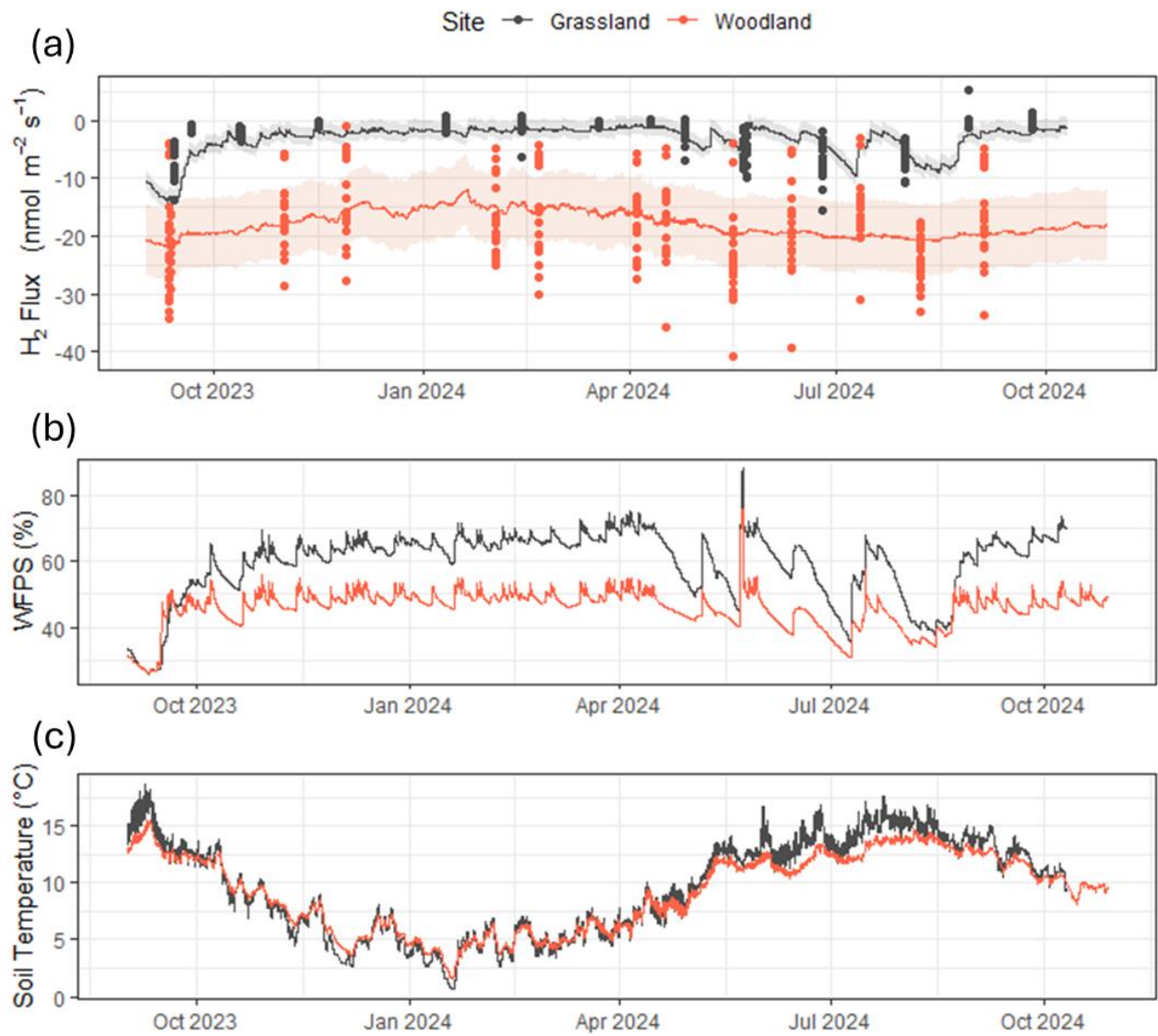
282 **Figure 3.** Correlations between H₂ flux and (a) water filled pore space (WFPS) and (b) Soil Temperature.

283 Correlations between CH₄ flux and (c) water filled pore space (WFPS) and (d) Soil Temperature. WFPS and soil

284 temperature measured at 10 cm depth via sampling probe. A 2nd order polynomial fit (black dashed line) is

285 included as a visual aid ($y = a_1x^2 + a_2x + c$) (Figure replicated for Vd in Figure S2).

286



287

288 **Figure 4.** (a) H_2 flux measurements and model predictions for both field sites using a multiple regression fit
 289 with soil moisture (x) and soil temperature (z) ($y = a_1x^2 + a_2x + b_1z^2 + b_2z + c$). (b) Continuous water filled pore
 290 space (WFPS) at measurements made at 10 cm depth (average of 60 mins). (c) Continuous soil temperature
 291 at measurements made at 10 cm depth (average of 60 mins).

292

4. Discussion

293

4.1. Quantification of H₂ flux

294 Fluxes of H₂ measured in this study range from -40.7 to 5.3 nmol m⁻² s⁻¹ with mean fluxes of -2.6 ± 0.4 and -
295 18.7 ± 1.0 nmol m⁻² s⁻¹ for the grassland and woodland sites, respectively. Using regression to model (gap-fill)
296 flux data, we estimate annual H₂ uptake of 3.1 ± 0.1 and 12.0 ± 0.4 kg H₂ ha⁻¹ yr⁻¹ for the grassland and
297 woodland sites, respectively, which increases the modelled mean uptake at the grassland site to 4.3 ± 0.2
298 nmol m⁻² s⁻¹ (in comparison to a measured mean uptake of 2.6 ± 0.4 nmol m⁻² s⁻¹) while the expected mean
299 uptake at the woodland site remains near 18 nmol m⁻² s⁻¹ (Table 3). Predicted uptake is higher at the grassland
300 site due to the expectation in the model that uptake will increase during periods of drier soils that were not
301 measured directly. Predicted uptake estimated by the model and the extrapolation of the mean flux are not
302 significantly different at the woodland site due to the lack of correlation with soil drivers in the model.
303 However, the model does predict that uptake will slow down during the coldest months when fewer
304 measurements were made at the site.

305 Mean measured uptake of H₂ at the grassland site is at the lower end of uptake reported in other studies that
306 directly measured H₂ flux from soils, which range from -1.5 to >20 nmol m⁻² s⁻¹ (Table 3). The mean soil uptake
307 of H₂ at the woodland site is at the higher end in terms of uptake magnitude, close in magnitude to high
308 deposition velocities reported for peatlands in Simmonds et al., (2011). While uptake at this site seems high,
309 we are confident that the flux measurements are accurate based on the consistency of flux observations and
310 the quality controls put in place. Concentrations of H₂ in the chambers consistently fell exponentially, reaching
311 near zero within 5 minutes (often within 3 mins) of enclosure. At the time of chamber closure (t₀), a volume
312 of 0.025 m³ of ambient air at the woodland site contains approximately 400-500 nmol of H₂ gas. To reach zero
313 within 5 mins would require fluxes approximately 10-12 nmol m⁻² s⁻¹ in magnitude. While dealing with the
314 exponential non-linearity of the rate of change of the concentration (dC/dt) does introduce an element of
315 uncertainty in the flux calculations, we are confident the method used in this study (HMR fitting) accurately
316 captures the flux at t₀ and thus a realistic magnitude of soil H₂ uptake.

317 Only two of the measured H₂ fluxes were both positive and larger than the analytical noise of the
318 measurement method. However, these measurements from separate chambers on separate dates (from the
319 grassland site) both showed 7 consecutive concentration measurements, all clearly increasing with time,
320 highlighting that it is possible for H₂ emissions to occur in soils, even where uptake is the predominant
321 direction of flux. It has been observed that legumes produce H₂ during the nitrogen fixation process (e.g.
322 Schubert and Evans 1976; Flynn et al., 2014); however, no legume plants were present in any of the chamber
323 locations during the study. The source of these H₂ emissions remains unknown and at no point did either of

324 the field sites become a source of H₂, but our observations do highlight that there remain unknown microbial
325 and geological processes at the sub-field scale.

326

327 **Table 3.** A summary of H₂ net fluxes and deposition velocity (Vd) measurements reported in literature,
328 compared with measured and modelled values in this study. Mean values and reported uncertainties. Where
329 only flux or Vd is reported, missing values are estimated using an ambient H₂ concentration of 500 ppb.

Study	Soil Type	Country	Mean H ₂ Flux (nmol m ⁻² s ⁻¹)	Mean Vd (cm s ⁻¹)
This study (measured)	Grass (Grazing)	UK (SCO)	-2.6 ± 0.4	0.012 ± 0.002
This study (gap-filled annual average)	Grass (Grazing)	UK (SCO)	-4.3 ± 0.2	
This study (measured)	Woodland	UK (SCO)	-18.2 ± 1.0	0.088 ± 0.005
This study (gap-filled annual average)	Woodland	UK (SCO)	-18.7 ± 0.6	
Smith-Downey et al. (2008)	Forest	USA (CA)	-7.9 ± 4.2	0.063 ± 0.029
	Desert	USA (CA)	-7.6 ± 5.3	0.051 ± 0.036
	Marsh	USA (CA)	-7.5 ± 3.4	0.035 ± 0.013
Lallo et al. (2009)	Urban park	FIN (Hesa)	-10.0 ± 2.5	0.020 ± 0.005
	Urban park	FIN (Hesa)	-19.0 ± 3.5	0.038 ± 0.007
Hammer and Levin (2009)	Urban/Agriculture	GER (BW)	-6.4 ± 1.6	0.03 ± 0.007
Simmonds et al. (2011)	Peatland	IRE (GAL)	-26.5	0.053
			(-9.0 – -64.5)	(0.018 – 0.129)
Meredith et al. (2017)	Woodland	USA (MA)	-3.2 ± 1.6	0.003 to 0.043
Baril et al. (2022)	Arable	CAN (QC)	-5.9 ± 4.3	0.012 ± 0.009
Buzzard et al. (2022)	Desert (Monsoon)	USA (AZ)	-1.5 to -3.5	0.03 to 0.007
Nagai et al. (2024)	Arable	JAP (JP02)	-5 to -10	0.01 to 0.02

330

331 **4.2. Drivers of H₂ flux**

332 This study provides evidence of large variability in H₂ flux behaviour across two different soil types and the
333 importance of environmental factors such as soil temperature and moisture content. At the grassland site,
334 soil moisture (WFPS) dominated the net H₂ flux behaviour in the soils. The relationship between H₂ uptake
335 and soil moisture was statistically significant ($p < 0.001$) and explained 60% of the variance observed in the
336 grassland H₂ fluxes observed. While H₂ flux does appear to correlate with soil temperature at the grassland
337 site when compared directly, this is almost entirely due to the strong correlation between soil moisture and
338 soil temperature ($R^2 = 0.68$). Multiple regression finds soil temperature to be an insignificant variable once
339 the effect of soil moisture is accounted for at the grassland site. Spatial variability in H₂ fluxes at the woodland
340 site were an order of magnitude higher than those at the grassland site. This spatial variability could not be
341 explained by soil moisture, temperature or the total carbon content of the soil. While there do appear to be

342 weak relationships between the flux data and soil moisture and soil temperature, neither is found to be
343 statistically significant (maximum p-value of 0.15 for soil temperature).

344 Meteorological conditions were almost identical at the local scale (sites are less than 3 km apart) and soil at
345 both sites was of a similar pH and had similar total carbon and nitrogen contents. A small difference in
346 ambient H₂ concentrations was observed between the sites which may be caused by the large soil uptake and
347 poorer circulation of air at the woodland site, resulting in lower near surface H₂ concentrations. The reason
348 for the large difference in flux of H₂ measured between the two sites is not entirely clear from the measured
349 data, but it is likely that the physical properties of the soils played a role. While rooting systems and carbon
350 structure within the surface layers of the soils will be different at the sites, one large and obvious disparity is
351 the silt/clay content of the soils which is approximately 75% and 40% at the grassland and woodland sites,
352 respectively. While both soils have similar particle density, the difference in silt/clay content implies variations
353 in pore size distribution and connectivity which will likely lead to different sensitivities to moisture changes.
354 We hypothesise from this assessment that the high fraction of silt/clay soil at the grassland site results in the
355 soil becoming highly anaerobic when moisture levels increase, as can be seen in the switching from CH₄
356 uptake to CH₄ emission when WFPS exceeded 40%. At the woodland site, a thin layer of organic materials
357 (forest litter that could provide a source of labile carbon) lies on top of a sandy, well-drained soil, which may
358 provide ideal conditions for H₂ uptake. Uptake of CH₄ is generally greater than at the grassland site, and WFPS
359 remains lower throughout the year, showing that drainage is significantly faster at the site and suggests that
360 the soils are more aerobic than at the grassland site (e.g. better penetration of H₂ to active regions within the
361 soil). While the differences in soil texture may partly explain the large magnitude of difference in H₂ uptake
362 between the sites, it does not account for the large spatial variability of H₂ flux at the woodland site. We
363 observe that the flux at the grassland site is largely dependent on physical factors at the field scale such as
364 the moisture content (aeration) of the soil, but the woodland site showed large variations between plots. This
365 variation may be due to microbial factors that are highly spatial in a forest floor, such as available nutrients
366 (labile carbon from rotting plant litter), canopy shading and varying microbial densities.

367

368 **4.3. Considerations for future research**

369 Chamber flux methods are commonplace in the field of GHG flux measurements, but there are several
370 important factors that need to be considered when carrying out H₂ flux measurements in the field. One of
371 the most important - when using gas chromatography analysis - is the lifetime of samples stored in vials due
372 to leakage rates from the rubber septum materials used to cap vials. While it is possible to keep GHG samples
373 in these vials for weeks or even months without significant storage loss, H₂ concentrations were found to
374 change relatively quickly, and should be analysed as soon as is possible (within 24 h of measurement). This

375 severely limits the reach of a particular field experiment to within travel distances of a working H₂ gas
376 chromatography instrument (e.g. not suitable for international shipment of samples). Almost all published H₂
377 flux measurements to date are within the temperate region of the northern hemisphere (USA and Europe),
378 which limits the available data for models to predict soil/atmosphere interactions at the global scale. Building
379 H₂ flux datasets at a global level would require either investment in localised infrastructure that allows for
380 samples to be analysed in-country, or for the deployment of temporary roving measurement methodology
381 which travels between sites. We emphasise that unless particular care and attention is applied to the
382 transportation of gas samples (e.g. tests and quality control checks), the H₂ flux cannot be analysed over a
383 large distance due to leakage of samples.

384 Field measurements of H₂ are beneficial due to realistic environmental conditions. However, the manual
385 aspects of chamber sampling create logistical issues (extensive fieldwork) and the overlap of many
386 environmental and soil variables can make it difficult to identify the driving forces behind H₂ flux (e.g. the soil
387 moisture/temperature comparison). With this setup, the GC-PDHID is limited to one gas sample every 4
388 minutes, thus auto-chambers (chambers that open/close and measure gas samples automatically) are limited
389 in capability. New faster instruments able to measure H₂ gas via infra-red spectroscopy (by converting H₂ to
390 H₂O) are becoming more commercially available (see aerodyne.com/laser-analyzers), but there are no studies
391 using these analysers to date. Previously gas chromatography instrumentation has been used to measure H₂
392 flux via the aerodynamic gradient method (Meredith et al., 2017), which allows half hourly fluxes to be
393 measured at the field scale. While micrometeorological methods such as the aerodynamic gradient method
394 allow for a greater temporal and spatial coverage of soil fluxes, they also require certain field conditions, such
395 as flat open terrain and large (mains) power supply. In the case of the woodland site in this study,
396 micrometeorological methods are not feasible. With current available H₂ measurement methods, care must
397 be given when planning measurement activities to ensure efficiency in data collection.

398 Lab-based incubation studies of H₂ flux in literature are similar in number to those measured in the field.
399 Incubation studies allow for better control of soil conditions such as moisture, temperature and nutrient
400 content, environmental conditions (air temperature) and also for consistency in microbial populations (via
401 replicates of well mixed/homogenised soils). For example, in this study, it was difficult to determine the
402 impact of soil temperature due to the correlation with soil moisture. Due to the climate in the region, there
403 were no periods when the soils were cold and also dry, preventing observations of different extremes of the
404 driving forces behind H₂ flux (see Figure S4). Incubation studies would be able to provide more information
405 on these drivers which may help modelling efforts; however, field measurements are still required to validate
406 flux models as incubation studies inevitably come with the caveat that flux measurements are not
407 representative of true soil conditions due to soil cores being repacked and creating therefore artificial
408 conditions.

409 **5. Conclusions**

410 This study reports that the soil sink (uptake) of H₂ for a grassland and a forest site in close proximity is -3.1 ±
411 0.1 and -12.0 ± 0.4 kg H₂ ha⁻¹ yr⁻¹, respectively (with mean Vds of 0.012 ± 0.002 and 0.088 ± 0.005 cm s⁻¹ for
412 grassland and forest soils, respectively). Soil moisture was found to be the primary driver of H₂ uptake at the
413 grassland site, where the high silt/clay content of the soil resulted in anaerobic conditions (near zero H₂ flux)
414 during wet periods of the year. Uptake of H₂ at the forest site was highly variable and did not correlate well
415 with any localised soil properties. Both sites were exposed to similar meteorological conditions (3 km apart)
416 and had similar basic soil properties (such as pH and carbon content), thus we conclude that the large
417 difference in uptake between the soils was dependent on soil aeration and diffusivity of H₂. It is likely that the
418 high silt/clay content of the grassland site (55%) resulted in a lack of aeration when soils were wet, while the
419 well-drained forest site (25% clay) was not restricted by exchange of H₂ between the atmosphere and the soil,
420 showing instead a large variability in H₂ flux that could be related to heterogeneous factors that control
421 microbial activity (e.g. labile carbon and microbial densities). In order to account for the large magnitude of
422 site-scale differences like those observed in this study, further field sites should be studied over a range of
423 soil and land cover types and management activities to improve global models of the soil H₂ sink. In addition,
424 laboratory incubations are needed to measure H₂ fluxes under controlled environmental conditions to refine
425 the main driving parameters of H₂ fluxes further.

426 **6. Acknowledgements**

427 Funding for this study has been provided by the UKRI Natural Environment Research Council (NERC) under
428 Grant Ref: NE/X013456/1 (Topic B: The Enigma of the Soil Hydrogen Sink Variability [ELGAR]). The work has
429 also been supported by the UK Research and Innovation (UKRI) Global Challenges Research Fund (GCRF) as
430 part of the South Asia Nitrogen Hub SANH project (NE/S009019/1).

431 **7. Competing interests**

432 The authors declare that they have no conflict of interest.

433 **8. Data availability**

434 Data currently undergoing preparation for submission to the Environmental Information Data Centre (EIDC).
435 <https://eidc.ac.uk/>

436

437 **9. Author contributions**

438 N. Cowan was the primary author of the manuscript and carried out all data analysis presented. The field
439 team that developed measurement methodology protocols, carried out measurements, maintained field
440 instrumentation and performed lab analysis consisted of T. Roberts, M. Hanlon, A. Bezanger, G. Toteva, A.
441 Tweedie, K. Yeung and A. Deshpande. The project management and significant contributors to the
442 manuscript text consisted of P. Levy, U. Skiba, E. Nemitz and J. Drewer. All coauthors contributed to the
443 writing of the manuscript before submission.

444

445 **10. References**

446 Baril, X., Durand, A.-A., Srei, N., Lamothe, S., Provost, C., Martineau, C., Dunfield, K., Constant, P., 2022. The
447 biological sink of atmospheric H₂ is more sensitive to spatial variation of microbial diversity than N₂O and
448 CO₂ emissions in a winter cover crop field trial. *Science of The Total Environment*.
449 <https://doi.org/10.1016/j.scitotenv.2022.153420>

450 Bertagni, M.B., Pacala, S.W., Paulot, F., Porporato, A., 2022. Risk of the hydrogen economy for atmospheric
451 methane. *Nat Commun.* <https://doi.org/10.1038/s41467-022-35419-7>

452 Billington, H.L. and Pelham, J., 1991. Genetic Variation in the Date of Budburst in Scottish Birch Populations:
453 Implications for Climate Change. *Functional Ecology*, 5(3), pp. 403–409. <https://doi.org/10.2307/2389812>.

454 Buzzard, V., Thorne, D., Gil-Loaiza, J., Cueva, A., Meredith, L.K., 2022. Sensitivity of soil hydrogen uptake to
455 natural and managed moisture dynamics in a semiarid urban ecosystem. *PeerJ*.
456 <https://doi.org/10.7717/peerj.12966>

457 Cooper, J., Dubey, L., Bakkaloglu, S., Hawkes, A., 2022. Hydrogen emissions from the hydrogen value chain-
458 emissions profile and impact to global warming. *Science of The Total Environment*.
459 <https://doi.org/10.1016/j.scitotenv.2022.154624>

460 Cowan, N., Levy, P., Maire, J., Coyle, M., Leeson, S.R., Famulari, D., Carozzi, M., Nemitz, E., Skiba, U., 2020. An
461 evaluation of four years of nitrous oxide fluxes after application of ammonium nitrate and urea fertilisers
462 measured using the eddy covariance method. *Agricultural and Forest Meteorology*.
463 <https://doi.org/10.1016/j.agrformet.2019.107812>

464 Cowan, N., Levy, P., Tigli, M., Toteva, G., Drewer, J., 2025. Characterisation of Analytical Uncertainty in
465 Chamber Soil Flux Measurements. *European J Soil Science*. <https://doi.org/10.1111/ejss.70104>

466 Derwent, R.G., Stevenson, D.S., Utembe, S.R., Jenkin, M.E., Khan, A.H., Shallcross, D.E., 2020. Global modelling
467 studies of hydrogen and its isotopomers using STOCHEM-CRI: Likely radiative forcing consequences of a
468 future hydrogen economy. International Journal of Hydrogen Energy.
469 <https://doi.org/10.1016/j.ijhydene.2020.01.125>

470 Deshpande, A.G., Jones, M.R., van Dijk, N., Mullinger, N.J., Harvey, D., Nicoll, R., Toteva, G., Weerakoon, G.,
471 Nissanka, S., Weerakoon, B., Grenier, M., Iwanicka, A., Duarte, F., Stephens, A., Ellis, C.J., Vieno, M., Dreher,
472 J., Wolseley, P.A., Nanayakkara, S., Prabhashwara, T., Bealey, W.J., Nemitz, E., Sutton, M.A., 2024.
473 Estimation of ammonia deposition to forest ecosystems in Scotland and Sri Lanka using wind-controlled
474 NH₃ enhancement experiments. Atmospheric Environment.
475 <https://doi.org/10.1016/j.atmosenv.2023.120325>

476 Dreher, J., Anderson, M., Levy, P.E., Scholtes, B., Helfter, C., Parker, J., Rees, R.M., Skiba, U.M., 2016. The
477 impact of ploughing intensively managed temperate grasslands on N₂O, CH₄ and CO₂ fluxes. Plant Soil.
478 <https://doi.org/10.1007/s11104-016-3023-x>

479 Dreher, J., Anderson, M., Levy, P.E., Scholtes, B., Helfter, C., Parker, J., Rees, R.M., Skiba, U.M., 2016. The
480 impact of ploughing intensively managed temperate grasslands on N₂O, CH₄ and CO₂ fluxes. Plant Soil.
481 <https://doi.org/10.1007/s11104-016-3023-x>

482 Ehhalt, D.H., Rohrer, F., 2009. The tropospheric cycle of H₂: a critical review. Tellus B: Chemical and Physical
483 Meteorology. <https://doi.org/10.1111/j.1600-0889.2009.00416.x>

484 Field, R.A., Derwent, R.G., 2021. Global warming consequences of replacing natural gas with hydrogen in the
485 domestic energy sectors of future low-carbon economies in the United Kingdom and the United States of
486 America. International Journal of Hydrogen Energy. <https://doi.org/10.1016/j.ijhydene.2021.06.120>

487 Flynn, B., Graham, A., Scott, N., Layzell, D.B., Dong, Z., 2014. Nitrogen fixation, hydrogen production and N₂O
488 emissions. Can. J. Plant Sci. <https://doi.org/10.4141/cjps2013-210>

489 Greening, C., Grinter, R., 2022. Microbial oxidation of atmospheric trace gases. Nat Rev Microbiol.
490 <https://doi.org/10.1038/s41579-022-00724-x>

491 Hammer, S., Levin, I., 2009. Seasonal variation of the molecular hydrogen uptake by soils inferred from
492 continuous atmospheric observations in Heidelberg, southwest Germany. Tellus B: Chemical and Physical
493 Meteorology. <https://doi.org/10.1111/j.1600-0889.2009.00417.x>

494 Hitchcock, W. K., Beamish, B. B. and Cliff D., 2019. A Study of the Formation of Hydrogen Produced During the
495 Oxidation of Bulk Coal Under Laboratory Conditions, in Naj Aziz and Bob Kininmonth (eds.), Proceedings
496 of the 2008 Coal Operators' Conference, Mining Engineering, University of Wollongong

497 Hutchinson, G.L., Mosier, A.R., 1981. Improved Soil Cover Method for Field Measurement of Nitrous Oxide
498 Fluxes. *Soil Science Society of America Journal.*
499 <https://doi.org/10.2136/sssaj1981.03615995004500020017x>

500 Islam, Z.F., Welsh, C., Bayly, K., Grinter, R., Southam, G., Gagen, E.J., Greening, C., 2020. A widely distributed
501 hydrogenase oxidises atmospheric H₂ during bacterial growth. *The ISME Journal.*
502 <https://doi.org/10.1038/s41396-020-0713-4>

503 Khalil, M.A.K., Rasmussen, R.A., 1990. The global cycle of carbon monoxide: Trends and mass balance.
504 *Chemosphere.* [https://doi.org/10.1016/0045-6535\(90\)90098-e](https://doi.org/10.1016/0045-6535(90)90098-e)

505 Field, R.A., Derwent, R.G., 2021. Global warming consequences of replacing natural gas with hydrogen in the
506 domestic energy sectors of future low-carbon economies in the United Kingdom and the United States of
507 America. *International Journal of Hydrogen Energy.* <https://doi.org/10.1016/j.ijhydene.2021.06.120>

508 Lallo, M., Aalto, T., Hatakka, J., Laurila, T., 2009. Hydrogen soil deposition at an urban site in Finland. *Atmos.*
509 *Chem. Phys.* <https://doi.org/10.5194/acp-9-8559-2009>

510 Meredith, L.K., Commane, R., Keenan, T.F., Klosterman, S.T., Munger, J.W., Templer, P.H., Tang, J., Wofsy, S.C.,
511 Prinn, R.G., 2016. Ecosystem fluxes of hydrogen in a mid-latitude forest driven by soil microorganisms and
512 plants. *Global Change Biology.* <https://doi.org/10.1111/gcb.13463>

513 Nagai, M., Kakiuchi, H., Masuda, T., 2024. Measurements of hydrogen deposition velocities by farmland soil
514 using D₂ gas. *Radiation Protection Dosimetry.* <https://doi.org/10.1093/rpd/ncae055>

515 Novelli, P.C., Lang, P.M., Masarie, K.A., Hurst, D.F., Myers, R., Elkins, J.W., 1999. Molecular hydrogen in the
516 troposphere: Global distribution and budget. *J. Geophys. Res.* <https://doi.org/10.1029/1999jd900788>

517 Ocko, I.B., Hamburg, S.P., 2022. Climate consequences of hydrogen emissions. *Atmos. Chem. Phys.*
518 <https://doi.org/10.5194/acp-22-9349-2022>

519 Paulot, F., Paynter, D., Naik, V., Malyshev, S., Menzel, R., Horowitz, L.W., 2021. Global modeling of hydrogen
520 using GFDL-AM4.1: Sensitivity of soil removal and radiative forcing. *International Journal of Hydrogen*
521 *Energy.* <https://doi.org/10.1016/j.ijhydene.2021.01.088>

522 Paulot, F., Pétron, G., Crotwell, A.M., Bertagni, M.B., 2024. Reanalysis of NOAA H₂ observations: implications
523 for the H₂ budget. *Atmos. Chem. Phys.* <https://doi.org/10.5194/acp-24-4217-2024>

524 Patterson, J.D., Aydin, M., Crotwell, A.M., Pétron, G., Severinghaus, J.P., Krummel, P.B., Langenfelds, R.L.,
525 Saltzman, E.S., 2021. H₂ in Antarctic firn air: Atmospheric reconstructions and implications for
526 anthropogenic emissions. *Proc. Natl. Acad. Sci. U.S.A.* <https://doi.org/10.1073/pnas.2103335118>

527 Pedersen, A.R., Petersen, S.O., Schelde, K., 2010. A comprehensive approach to soil-atmosphere trace-gas
528 flux estimation with static chambers. European J Soil Science. <https://doi.org/10.1111/j.1365-2389.2010.01291.x>

530 Petron, G. B., Crotwell, A. M., Mund, J., Crotwell, M., Mefford, T., Thoning, K., Hall, B. D., Kitzis, D. R.,
531 Madronich, M., Moglia, E., Neff, D., Wolter, S., Jordan, A., Krummel, P., Langenfelds, R., and Patterson, J.
532 D.: Atmospheric H₂ observations from the NOAA Global Cooperative Air Sampling Network, Atmos. Meas.
533 Tech. Discuss. [preprint], <https://doi.org/10.5194/amt-2024-4>, in review, 2024.

534 Piché-Choquette, S., Constant, P., 2019. Molecular Hydrogen, a Neglected Key Driver of Soil Biogeochemical
535 Processes. Appl Environ Microbiol. <https://doi.org/10.1128/aem.02418-18>

536 Saavedra-Lavoie, J., de la Porte, A., Piché-Choquette, S., Guertin, C., Constant, P., 2020. Biological H₂ and CO
537 oxidation activities are sensitive to compositional change of soil microbial communities. Can. J. Microbiol.
538 <https://doi.org/10.1139/cjm-2019-0412>

539 Sand, M., Skeie, R.B., Sandstad, M., Krishnan, S., Myhre, G., Bryant, H., Derwent, R., Hauglustaine, D., Paulot,
540 F., Prather, M., Stevenson, D., 2023. A multi-model assessment of the Global Warming Potential of
541 hydrogen. Commun Earth Environ. <https://doi.org/10.1038/s43247-023-00857-8>

542 Schubert, K.R., Evans, H.J., 1976. Hydrogen evolution: A major factor affecting the efficiency of nitrogen
543 fixation in nodulated symbionts. Proc. Natl. Acad. Sci. U.S.A. <https://doi.org/10.1073/pnas.73.4.1207>

544 Simmonds, P.G., Derwent, R.G., Manning, A.J., Grant, A., O'doherty, S., Spain, T.G., 2011. Estimation of
545 hydrogen deposition velocities from 1995–2008 at Mace Head, Ireland using a simple box model and
546 concurrent ozone depositions. Tellus B: Chemical and Physical Meteorology.
547 <https://doi.org/10.1111/j.1600-0889.2010.00518.x>

548 Smith-Downey, N.V., Randerson, J.T., Eiler, J.M., 2008. Molecular hydrogen uptake by soils in forest, desert,
549 and marsh ecosystems in California. J. Geophys. Res. <https://doi.org/10.1029/2008jg000701>

550 Warwick, N.J., Bekki, S., Nisbet, E.G., Pyle, J.A., 2004. Impact of a hydrogen economy on the stratosphere and
551 troposphere studied in a 2-D model. Geophysical Research Letters. <https://doi.org/10.1029/2003gl019224>

552

553